Biomaterials 134 (2017) 13–21

Contents lists available at ScienceDirect

Biomaterials

journal homepage: www.elsevier.com/locate/biomaterials

# Local delivery of chondroitinase ABC with or without stromal cell-derived factor 1α promotes functional repair in the injured rat spinal cord

Malgosia M. Pakulska [a, b], Charles H. Tator [d, e], Molly S. Shoichet [a, b, c, *]

[a] Department of Chemical Engineering and Applied Chemistry, University of Toronto, Toronto, ON, M5S 3E5, Canada
[b] Institute for Biomaterials and Biomedical Engineering, University of Toronto, Toronto, ON, M5S 3G9, Canada
[c] Department of Chemistry, University of Toronto, Toronto, ON, M5S 3H6, Canada
[d] Krembil Research Institute, University Health Network, Toronto, ON, M5T 1M8, Canada
[e] Department of Surgery, University of Toronto, Toronto, ON, M5T 1P5, Canada

ARTICLE INFO

*Article history:*
Received 25 January 2017
Received in revised form
10 April 2017
Accepted 12 April 2017
Available online 18 April 2017

*Keywords:*
Hydrogel
Chondroitinase ABC
Stromal cell derived factor
Spinal cord injury
Controlled release
Affinity release
Methylcellulose

ABSTRACT

Traumatic spinal cord injury (SCI) is a devastating event for which functional recovery remains elusive. Due to the complex nature of SCI pathology, a combination treatment strategy will likely be required for success. We hypothesized that tissue and functional repair would be achieved in a rat model of impact-compression SCI by combining degradation of the glial scar, using chondroitinase ABC (ChABC), with recruitment of endogenous neural precursor cells (NPCs), using stromal cell-derived factor 1α (SDF). To test this hypothesis, we designed a crosslinked methylcellulose hydrogel (XMC) for minimally invasive, localized, and sustained intrathecal drug delivery. ChABC was released from XMC using protein-peptide affinity interactions while SDF was delivered by electrostatic affinity interactions from polymeric nanoparticles embedded in XMC. Rats with SCI were treated acutely with a combination of SDF and ChABC, SDF alone, ChABC alone, or vehicle alone, and compared to injury only. Treatment with ChABC, both alone and in combination with SDF, resulted in faster and more sustained behavioural improvement over time than other groups. The significantly reduced chondroitin sulfate proteoglycan levels and greater distribution of NPCs throughout the spinal cord tissue with ChABC delivery, both alone and in combination with SDF, may explain the improved locomotor function. Treatment with SDF alone had no apparent effect on NPC number or distribution nor synergistic effect with ChABC delivery. Thus, in this model of SCI, tissue and functional repair is attributed to ChABC.



## 1. Introduction

Traumatic spinal cord injury (SCI) results in a devastating loss of sensory and motor function with no current drug treatments that can consistently restore function. Although there is some spontaneous regenerative response following SCI, it is insufficient for meaningful recovery. For example, axons will form new growth cones shortly after injury; however, the lack of guidance information and the presence of inhibitory molecules, including the glial scar, causes growth to arrest, resulting in dystrophic end bulbs [1,2]. Similarly, a spontaneous regenerative response that includes activation, proliferation, and migration of endogenous neural precursor cells (NPCs) from the ependyma of the central canal to the injury site is initiated after injury [3], but does not induce meaningful functional recovery. Regenerative therapies that can both extend or amplify the endogenous regenerative response and mitigate the inhibitory injury environment are promising treatment options.

Stromal cell-derived factor 1α (SDF) is a chemokine that plays a critical role in the development of the central nervous system (CNS) and is increasingly considered a major effector of endogenous neural precursor cell (NPC) migration after injury [4]. The ependymal cells lining the central canal, where multipotent neural stem cells reside in the rodent spinal cord [5,6], express the SDF receptor CXCR4 [7] and increased SDF expression has been correlated with NPC homing to sites of brain and spinal cord injury [8,9]. In vitro,

* Donnelly Centre for Cellular & Biomolecular Research, University of Toronto160 College Street, Room 530, Toronto, ON, M5S 3E1, Canada
*E-mail address:* molly.shoichet@utoronto.ca (M.S. Shoichet).

http://dx.doi.org/10.1016/j.biomaterials.2017.04.016
0142-9612/

SDF promotes NPC migration in a concentration dependent manner [9,10]. Moreover, intrathecal infusion of SDF at the site of SCI improved BBB scores in rats compared to vehicle controls after 7 days [11].

Chondroitinase ABC (ChABC) is an enzyme that degrades the sulfated glycosaminoglycan chains on the chondroitin sulfate proteoglycans (CSPGs) that are a major inhibitory component of the glial scar. Degradation of the glial scar has been shown to promote axonal growth resulting in functional recovery in rodent models of SCI [12]. ChABC also degrades the CSPGs that form perineuronal nets, thereby enhancing axonal sprouting and plasticity [13]. Combining ChABC with cell transplant improves migration and survival of the transplanted cells, and functional recovery [14–16]. We hypothesized that co-delivering ChABC and SDF would increase endogenous neural precursor cell homing to the injury site and improve their survival and distribution within the tissue.

As both ChABC and SDF suffer from short half-lives *in vivo,* multiple injections or prolonged release strategies are required. SDF is quickly cleaved into a truncated, inactive form by MMP2 [17], which is upregulated after SCI [18]. ChABC is thermally unstable [19] and remains active for less than 4 days within tissue [20]. To sustain release, ChABC and SDF are usually delivered by multiple bolus intrathecal injections or intrathecal infusion; however, these methods are invasive and prone to complications and infection when an external catheter is used [21]. Alternative strategies based on affinity and electrostatic interactions have recently emerged to control local release of these two molecules, obviating the need for the catheter/minipump system [22–24]. By taking advantage of the affinity between Src homology 3 (SH3) and its binding peptides, sustained release of bioactive ChABC was achieved *in vitro* for at least 7 days [22]. Briefly, a fusion protein of ChABC-SH3 with kinetic activity identical to unmodified ChABC was released from a crosslinked methylcellulose (XMC) hydrogel modified with SH3 binding peptides. Release of His-SH3-ChABC-FLAG was quantified using a double-tag ELISA with the N-terminal His-tag binding to a nickel-coated plate and the C-terminal FLAG tag detected using an anti-FLAG antibody. Thus, only intact, full-length ChABC-SH3 was detected. The released ChABC-SH3 fusion was active over the entire 7-day release period. By taking advantage of the transient electrostatic interactions between negatively charged poly(lactic-co-glycolic acid) (PLGA) nanoparticles (np) and positively charged SDF, the controlled release of bioactive SDF was achieved for at least 14 days, thereby eliminating the need for SDF encapsulation [24].

Here, we test, for the first time, the co-delivery of ChABC and SDF in a rat model of impact-compression SCI. ChABC and SDF are both released from an injectable, biocompatible XMC hydrogel by affinity and electrostatic mechanisms respectively, after acute SCI via minimally invasive, intrathecal injection. We examine tissue and functional recovery, including endogenous chondroitin sulfate proteoglycan (CSPG) expression and NPC distribution.

## 2. Materials and methods

### 2.1. Preparation of crosslinked MC (XMC) with SDF or ChABC-SH3

XMC was prepared as described previously [25]. Briefly, thiolated MC (MC-SH) [26] and unmodified MC (300 kDa, Shin-Etsu Corp.) were dissolved in artificial cerebrospinal fluid (aCSF: 350 mM NaCl, 3 mM KCl, 0.8 mM $MgCl_2$, 1.4 mM $CaCl_2$, 1.5 mM $Na_2HPO_4$, 0.2 mM $NaH_2PO_4$) to obtain a final concentration of 5% w/v total MC and 0.1 μmol thiol/100 μl gel. The gel was crosslinked using poly(ethylene glycol)-bismaleimide ($PEGMI_2$, 3000 Da, Rapp Polymere, Tuebingen, Germany) for a final molar ratio of 0.75:1 maleimide to thiol. For SDF-loaded gels, poly(lactic-co-glycolic acid) nanoparticles (np) (10% wt/v) [27] and recombinant mouse SDF1α (R&D Systems) (2.5 μg/5 μl) were added to the XMC prior to crosslinking. For ChABC gels, SH3 binding peptide-modified MC (MC-pep) [26] and recombinant ChABC-SH3 fusion protein [22] were added to XMC prior to crosslinking for a final ChABC-SH3 concentration of 0.3 U/5 μl and a final molar ratio of 1:100 ChABC-SH3:SH3 binding peptide.

### 2.2. Spinal cord injuries and treatment

Animal procedures were performed in accordance with the Guide to the Care and Use of Experimental Animals developed by the Canadian Council on Animal Care and approved by the Animal Care Committee at the Research Institute of the University Health Network.

#### 2.2.1. ChABC-SH3 penetration study

18 female Sprague Dawley rats (200–250 g; Charles River, Montreal, Canada) were anesthetized by inhalation of 2.5% isoflurane, and a laminectomy was performed at the T1-2 vertebral level. A moderate impact-compression injury was induced using a modified aneurysm clip (24.5 g) for 1 min [28].

Immediately after injury, a durotomy rostral to the injury site was performed with a 30 gauge, bent beveled needle. 10 μl of 5% w/v MC-peptide containing 350 mM NaCl or 10 μl of 5% w/v MC-peptide containing 350 mM NaCl and 10 μg ChABC-SH3 was injected through a 30 gauge, bent blunt-tipped needle into the intrathecal space in a caudal direction. The needle was held in place for 1 min before removal.

Following injection, the overlying muscles and fascia were sutured closed with Vicryl 3-0, and the rats were placed under a heat lamp for recovery. Buprenorphine (0.03 mg/kg) was administered every 12 h for 3 days postsurgery for pain management.

Animals were grouped as follows: MC-pep ($n = 6$) and MC-pep/ChABC ($n = 12$) and used for the tissue ELISA described below.

#### 2.2.2. For tissue ELISA

2 animals from the control group and 4 animals from the ChABC-SH3 treated group were sacrificed at each of 2, 7, and 28 days post injury and treatment. A 2 cm length of spinal cord from each animal encompassing the injury site (observed as a darker, brown, area on the cord) was harvested and frozen for processing. Using a tissue chopper, each cord was cut parasagitally into 1 mm wide pieces. The two central pieces from each cord were embedded in cryomatrix and sectioned using a cryostat into 100 μm dorso-ventral sections. Five of these sections were combined into 1 tube to obtain tissue from 500 μm dorso-ventral depth for analysis by ELISA.

#### 2.2.3. ChABC/SDF combination therapy

75 female Sprague Dawley rats (200–250 g; Charles River, Montreal, Canada) were anesthetized by inhalation of 2.5% isoflurane, and a laminectomy was performed at the T1-2 vertebral level. A moderate impact-compression injury was performed as described above.

Immediately after injury, a durotomy rostral to the injury site was performed with a 30 gauge, bent beveled needle. 5 μl of blank XMC-peptide or XMC-peptide containing ChABC-SH3 was injected through a 30 gauge, bent blunt-tipped needle into the intrathecal space in a caudal direction, as described above. The needle was held in place for 1 min before removal. A second durotomy was performed caudal to the injury site in the same way. 5 μl of XMC containing PLGA np or PLGA np and SDF was injected into the intrathecal space in a rostral direction such that the two gels localized at the injury site. The needle was held in place for 1 min before removal. Following the injections, the overlying muscles and

fascia were sutured closed with Vicryl 3-0, and the rats were placed under a heat lamp for recovery. Buprenorphine (0.03 mg/kg) was administered every 12 h for 3 days postsurgery for pain management.

Animals were grouped as follows (n = 15 per group): XMC-pep + XMC/PLGA np/SDF; XMC-pep/ChABC + XMC/PLGA np; XMC-pep/ChABC + XMC/PLGA/SDF np; XMC-pep + XMC/PLGA np; Injury only.

#### 2.2.4. For immunohistochemistry

4 animals from each group were sacrificed 2 weeks post injury and the remainder were sacrificed 8 weeks post injury. Animals were perfused intracardially with 4% paraformaldehyde in 0.1 M phosphate buffer under deep anesthesia. A 1.5 cm section of cord encompassing the injection site was harvested from each animal. A 0.5 cm section of cord encompassing the injury site (observed as a darker, brown, area on the cord) was cryoprocessed and cut into 20 μm cross-sections for staining. Sections were stored at −80 °C.

### 2.3. BBB score and BBB motor subscore

General locomotor performance was evaluated weekly for 8 weeks for 11 animals from each group using the Basso, Beattie and Bresnahan (BBB) 21-point scoring scale [29] and the BBB motor subscore 7-point scoring scale [30]. Each hindlimb was ranked by two blinded observers. Scores reflect the average of the two hindlimb scores for each animal.

### 2.4. Ladder walk

Prior to surgery, animals were handled daily for 5 days and familiarized with the ladder walk [31] every second day for a total of 3 days each. After surgery and treatment, animals with a BBB score of 11 or higher (reflecting occasional weight supported stepping and forelimb-hindlimb coordination) were tested on the ladder walk if they achieved BBB scores of 11 or higher. Rungs were spaced irregularly and the rung arrangement was changed every week to avoid confounding with learning or memory. Each animal performed the ladder walk task until 3 uninterrupted runs were obtained (no pauses). Runs were videotaped and the number of hindlimb foot faults was counted by a blinded observer. A foot fault was counted if the ankle of the animal passed below the level of the ladder rungs. The score for each animal reflects the average of 3 runs.

### 2.5. Tissue processing

#### 2.5.1. Tissue ELISA

Each tube containing a 500 μm dorso-ventral depth tissue section received 400 μl ammonium acetate, pH 8.0 and 4 autoclaved silica beads. Tissue was homogenized in a bead beater for 1 min, placed on ice for 2 min and homogenized again for 1 min. Tissue was pelleted in a microcentrifuge at 14,000 rpm for 20 min at 4 °C. An in-house HIS/FLAG ELISA was used to analyze the supernatant. 200 μl of ChABC-SH3 protein sample or known standard was added to each well of a Hisorb Ni-NTA 96-well plate (Qiagen, Toronto, ON) and incubated for 2 h at 37 °C on an orbital shaker. The wells were then washed with 250 μl 1× PBS +0.05% Tween-20 three times for 10 s each with vigorous tapping and blotted dry on paper towels. 200 μl of anti-FLAG antibody (Abcam ab21536) diluted 1:5000 in 1X PBS + 0.2% BSA was added to each well and incubated at 37 °C for 2 h on an orbital shaker. The wells were then washed as above and blotted dry. 200 μl of goat anti-rabbit IgG secondary antibody coupled with HRP (Abcam ab97051) diluted 1:10000 in 1X PBS + 0.2% BSA was added to each well and incubated at room temperature for 45 min on an orbital shaker. 100 μl of 2,2'-azino-bis(3-ethylbenzothiazoline-6-sulphonic acid) (ABTS) was then added to each well and incubated at room temperature for 10 min on an orbital shaker. The absorbance was measured at 405 nm with a wavelength correction at 650 nm. Tissue from control animals was also spiked with ChABC-SH3 and processed in the same way to use as the ELISA standard. Protein concentration was calculated based on the linear range of the standard curve from the same plate. Protein samples were diluted to fit within this linear range. Tissue from control animals was processed the same way and used as a blank.

#### 2.5.2. Tissue staining

The following primary antibodies were used at the indicated dilutions: mouse monoclonal anti-chondroitin sulfate clone CS-56 (Sigma C8035, 1:100), chicken polyclonal to GFAP (Abcam ab4674, 1:500), rabbit polyclonal to Ki67 (Abcam ab15580, 1:500), mouse monoclonal to Sox2 (Abcam ab79351, 1:500), ED-1 (Serotec-BioRad MCA341A488, 1:1000), CD206 (Abcam ab64693, 1:5000). The following secondary antibodies were used at a 1:500 dilution: goat anti-mouse IgM heavy chain Alexa Fluor 568 (Thermo Fisher A21043), goat anti-rabbit IgG Alexa Fluor 488 (Thermo Fisher A11034), goat anti-mouse IgG Alexa Fluor 647 (Thermo Fisher A21236), goat anti-chicken IgY Alexa Fluor 568 (Abcam ab175711). Sections were stained for CSPG, co-stained for Ki67, Sox2, and GFAP, or co-stained for ED-1 and CD206.

Before staining, slides were allowed to equilibrate to room temperature for 15 min and rehydrated with 0.1 M PBS with Tween 20 (PBST) for 5 min at room temperature. Slides were incubated with primary antibodies diluted in PBST overnight at 4 °C. Slides were washed with PBST 3 times, 5 min each, and incubated with secondary antibodies and 4′,6-damidino-2-phenylindole (DAPI, Life Technologies) diluted in PBST for 3 h at room temperature. Slides were washed with PBST 3 times, 5 min each and coverslipped with ProLong Gold anti-fade reagent (Life Technologies).

#### 2.5.3. Microscopy

Overviews of the samples stained for CSPG were taken using an inverted Olympus laser scanning confocal microscope equipped with a motorized stage at 20× magnification. Settings were adjusted with a blank slide (processed identically but with no primary antibodies) on each imaging day.

Samples stained for Ki67/Sox2/GFAP were imaged at 10× magnification using the slide scanning services at Huron Digital Pathology (Waterloo, ON).

Samples stained for ED-1/CD206 were imaged at 20× magnification using the slide scanning services at the University of Toronto Microscopy Imaging Laboratory.

4 slides with 8 sections each were imaged for each animal. Sections were 160 μm apart spanning approximately 2800 μm rostral and caudal to the injury epicentre.

#### 2.5.4. Image analysis and quantification

CSPG, GFAP, and cavity size were analyzed using Fiji software [32]. Each section was traced in the DAPI channel to determine the tissue area and cavity area. Cavity area was traced as the areas devoid of cells. Sections were converted to black and white using Fiji built-in threshold algorithms. Percent positive area normalized for the total tissue area was taken as the staining intensity for each antibody. Sections that were folded or ripped were excluded from analysis.

Cell counts were done using Imaris software (Bitplane) on two sections rostral and two sections caudal to the injury site that still contained an intact central canal (between 1500 μm and 2500 μm from the injury epicentre depending on the animal). Colocalization

was performed between the Ki67 and DAPI channels (Ki67 + cells) and the Sox2 and DAPI channels (Sox2 positive cells). A spots group was created for each colocalization channel. Ki67 + spots that colocalized with Sox2+ spots were counted as double positive cells and manually verified. A GFAP threshold was created by placing 3 measurement points in areas that were considered to have background GFAP staining intensity and the GFAP intensity at these 3 points was averaged to obtain the GFAP background level. Spots that were in areas below this background level were counted as Ki67+/Sox2+/GFAP-. These spots were also manually verified. A similar method was employed to quantify ED1+, CD206+, and ED1+/CD206 positive cells.

#### 2.5.5. Statistical analysis

Statistical analysis was done using GraphPad Prism software (San Diego, USA). Tests were done using two-way, repeated measures ANOVA with Tukey's or Dunnett's post hoc test or one-way ANOVA with Holm-Sidak's post-hoc test with $\alpha = 0.1$. The exact test used is described in the caption for each figure.

## 3. Results

### 3.1. Tissue penetration

Prior to studying the combined efficacy of ChABC and SDF, we first tested the diffusion of ChABC-SH3 from its injection site in the intrathecal space into the spinal cord tissue. We focused on ChABC sustained release (and not SDF) because ChABC has a significantly larger molar mass of 131 kDa vs. 8 kDa for SDF and we have previously demonstrated tissue penetration of proteins of similar molar mass and pI to SDF [33,34]. ChABC-SH3 was dispersed in the MC-based hydrogel modified with the SH3-binding peptide, KPPVVKKPHYLS, and injected into the dorsal intrathecal space at the time and site of injury. To measure ChABC tissue penetration, the spinal cord was dissected and dorsolateral serial sections at every 500 μm were combined, processed, and analyzed by ELISA for ChABC. At both 1 and 7 days after intrathecal gel injection, intact ChABC was detected at all depths within the spinal cord (Fig. 1A and B), but was detectable only on the surface of the cord 28 days after injection (Fig. 1C). Overall, we were able to detect over 10% of the injected dose within the cord over 28 days (Fig. 1D). Given that we examined the tissue for ChABC at three specific timepoints, our goal was not to account for all of the ChABC delivered, but rather to determine whether it persisted in the cord for a prolonged period of time.

### 3.2. ChABC promotes early and sustained behavioural improvement

To test the combination of controlled ChABC and SDF delivery, we injected XMC-SH3-binding peptide (XMC-pep) with ChABC-SH3 and/or composite XMC with PLGA np and SDF into the intrathecal space at the lesion site. Animals received one of: (1) XMC containing PLGA np and SDF plus XMC-pep containing ChABC-SH3 (referred to as SDF + ChABC), (2) XMC containing PLGA np and SDF (SDF), (3) XMC-pep containing ChABC-SH3 (ChABC), or 4) vehicle of XMC-pep and XMC + PLGA np (vehicle). An additional group of animals received injury alone with no treatment (injury only).

Animals were tested weekly for BBB locomotor score [29], BBB motor subscore [30], and on the ladder walk test. First, animals within each group were analyzed for improvement over time (Fig. 2A and B). For the motor subscore, only ChABC treated groups show significant within-group improvement compared to one week post-injury and treatment (Fig. 2A). Similarly, only ChABC treated animals show immediate significant and sustained within-

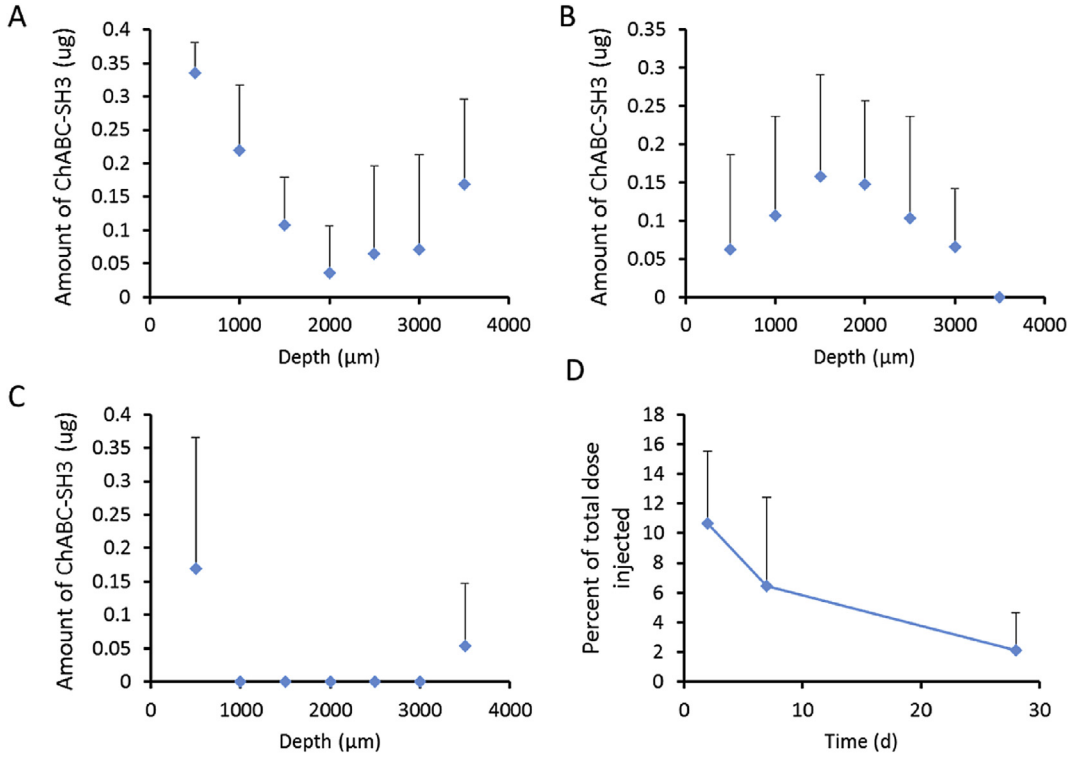


**Fig. 1. ChABC-SH3 released from an intrathecal, methylcellulose hydrogel penetrates dorsolaterally throughout the spinal cord and persists for 7 to 28 days**. The amount of ChABC detected via ELISA at various depths within the spinal cord at: A) 2, B) 7, and C) 28 days after injury and gel injection. 0 represents the dorsal side of the cord where the gel was injected. The rat spinal cord is about 3.5 mm in diameter. D) Percent of total injected ChABC-SH3 detectable within the entire section of cord. (n = 4 animals per timepoint, Mean + SD plotted).

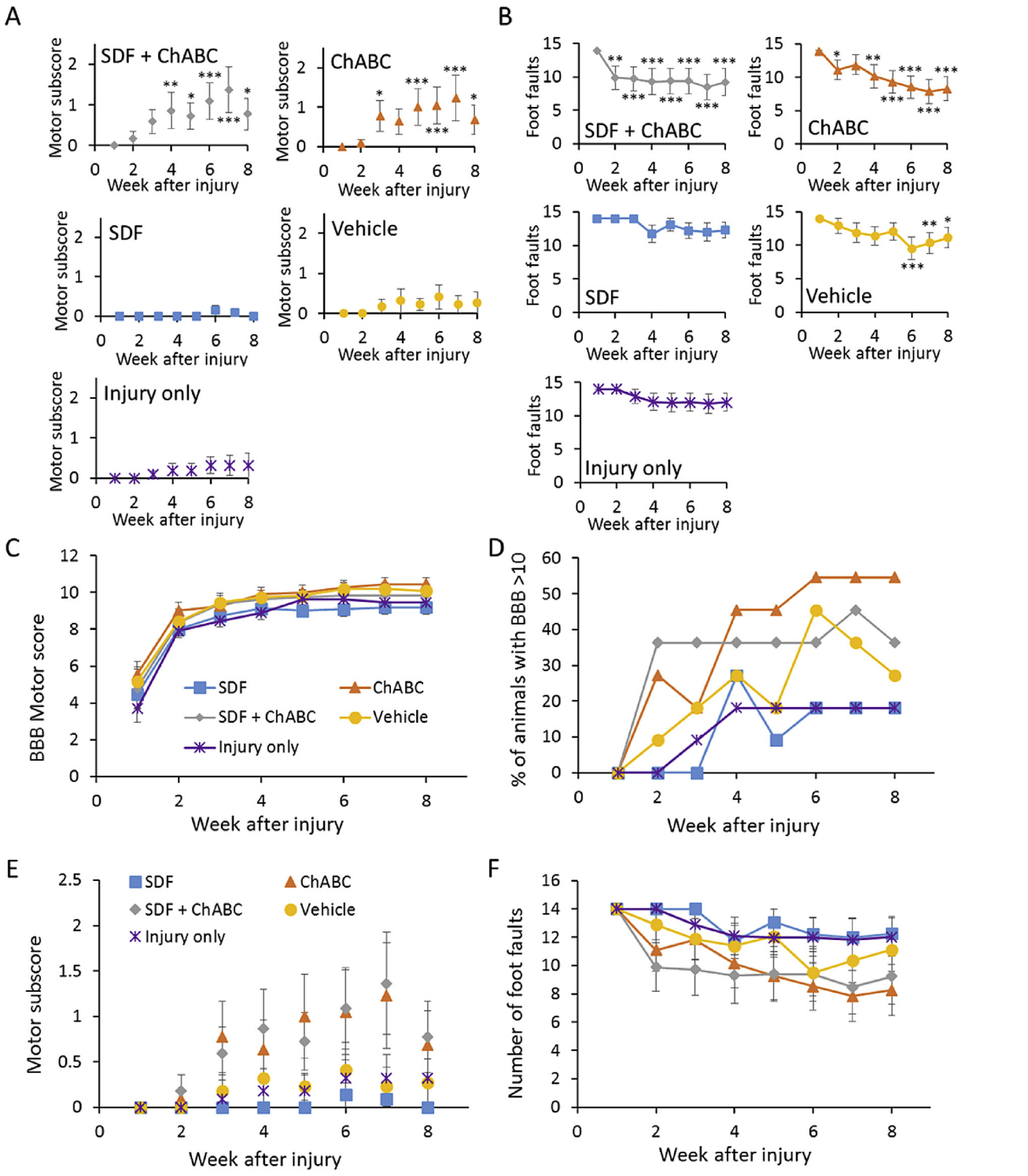


**Fig. 2. Application of ChABC results in early and persistent improvement in fine motor skills.** Compared to the first week after injury, only ChABC treated groups show significant within-group recovery in terms of both A) motor subscore, and B) ladderwalk. C) No significant differences are seen between groups in the BBB scores; however, D) ChABC treated groups show a higher percentage of animals with BBB scores above ten (weight supported stepping). No significant differences are seen between groups for the E) motor subscore or F) ladderwalk tasks. (n = 11 animals per group. Mean ± SEM plotted. *p < 0.05, **p < 0.005, ***p < 0.001. A, B: significant differences by repeated measures two-way ANOVA with Dunnett's post-hoc test compared to week one. C, E, F: significant differences by repeated measures two-way ANOVA with Tukey's post-hoc test).

group improvement in the ladder walk test over time (Fig. 2B). None of the other groups showed improvement over time with the motor subscore or ladderwalk tests, except the vehicle group, where some spontaneous recovery was observed 6 weeks after injury in the ladderwalk test, which was much later than the recovery observed in the ChABC-treated groups. No significant differences were observed between groups at any timepoint (Fig. 2C–F); however, there was a trend towards better performance in both the SDF + ChABC and ChABC groups, which had more animals with BBB scores > 10 (weight bearing steps) (Fig. 2D),

the highest motor subscores (Fig. 2E), and the fewest footfalls (Fig. 2F).

### 3.3. ChABC decreases chondroitin sulfate proteoglycan (CSPG) levels for at least 2 weeks

ChABC is known to degrade the glycosaminoglycan chains of the CSPGs that make up the glial scar. We therefore stained for total CSPG content at 2 and 8 weeks to test whether our new delivery strategy also had this effect (Fig. 3). CSPG staining was most intense around the injury epicenter with observed decreases right at the epicentre likely due to the loss of fragile tissue within the cavity during processing (Supplementary Fig. S1). For statistical analysis, values were averaged 800 μm rostral and caudal from the injury epicenter. At 2 weeks post injury, animals treated with ChABC (ChABC and SDF + ChABC groups), showed a significant decrease in average CSPG staining intensity compared to the vehicle control. The SDF group showed a significant increase in average CSPG levels compared to all other groups at 2 weeks post injury. There were no significant differences in CSPG levels between groups 8 weeks after injury. These data suggest that ChABC was bioactive in the injured spinal cord for at least 2 weeks, but not 8 weeks, after a single injection of the affinity release hydrogel into the intrathecal space.

We next stained for GFAP, since astrocytes are one of the major contributors to glial scar formation. GFAP staining was also used to determine cavity size, a common outcome measure after SCI studies. There were no significant differences in GFAP staining intensity or cavity size at 2 or 8 weeks post injury among any of the groups (Supplemental Fig. S2).

### 3.4. ChABC promotes NPC distribution throughout the spinal cord

As SDF has been shown to be a chemoattractant for NPCs, we analyzed the tissue for proliferating NPCs 2 weeks post injury in two sections rostral and two sections caudal to the injury site that contained an intact central canal. Cells were identified as proliferating NPCs if they stained positive for both Ki67 and Sox2 and negative for GFAP. Cells that were Ki67+/Sox2+/GFAP+ were counted as proliferating astrocytes and were not included in the analysis. The distribution of proliferating NPCs within the spinal cord was also analyzed by measuring the distance of each cell from the central canal (Fig. 4A and B). ChABC-treated animals had proliferating NPCs that were distributed significantly farther from the central canal than animals that received no treatment or those that received SDF only (Fig. 4A). The position of all the cells with respect to the central canal is visualized in Fig. 4B. The reduced CSPGs observed in ChABC-treated groups may explain the greater distance of NPCs observed in ChABC groups. No significant differences were observed in the total number of proliferating NPCs between any of the groups (Fig. 4C), suggesting that SDF did not stimulate NPCs. Representative tissue staining shows how the analysis was achieved (Fig. 4D).

Since SDF is also a macrophage stimulating molecule, we investigated the number of microglia/macrophages as well as the ratio of alternatively activated M2-type macrophages to total macrophages in each animal. No differences were observed between groups in either measure (Supplementary Fig. S3).

## 4. Discussion

Spinal cord injury has a complex pathophysiology, thus a combinatorial therapy will likely be required in order to achieve substantial functional benefit. In this study, we combined ChABC, an enzyme that can degrade inhibitory components of the glial scar, with SDF, a chemokine implicated in the migration of endogenous

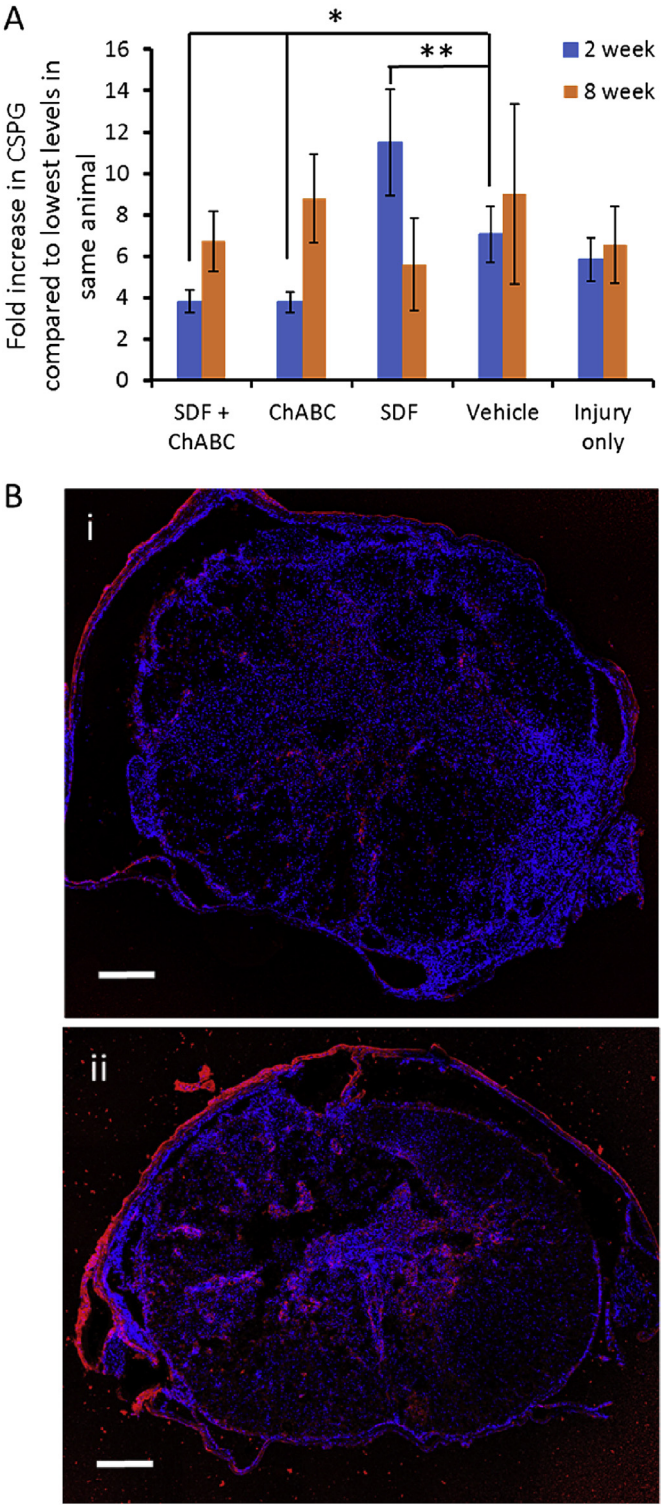


**Fig. 3. Local delivery of ChABC-SH3 from XMC-pep intrathecal injection results in decreased CSPG levels in spinal cord tissue.** A) Quantification of immunostained tissue shows a significant decrease in CSPG levels in ChABC treated groups compared to vehicle at 2 weeks, but not 8 weeks, after injury. (n = 4 animals per group, mean ± SD plotted. *$p < 0.05$, **$p < 0.005$. Significant differences by one-way ANOVA with Holm-Sidak's post-hoc test). B) Representative immunostained images of spinal cord tissue in cross-section from i) ChABC treated group and ii) vehicle treated group 2 weeks after injury at the injury epicentre (blue = DAPI, red = CSPG). Scale bars = 300 μm. (For interpretation of the references to colour in this figure legend, the reader is referred to the web version of this article.)

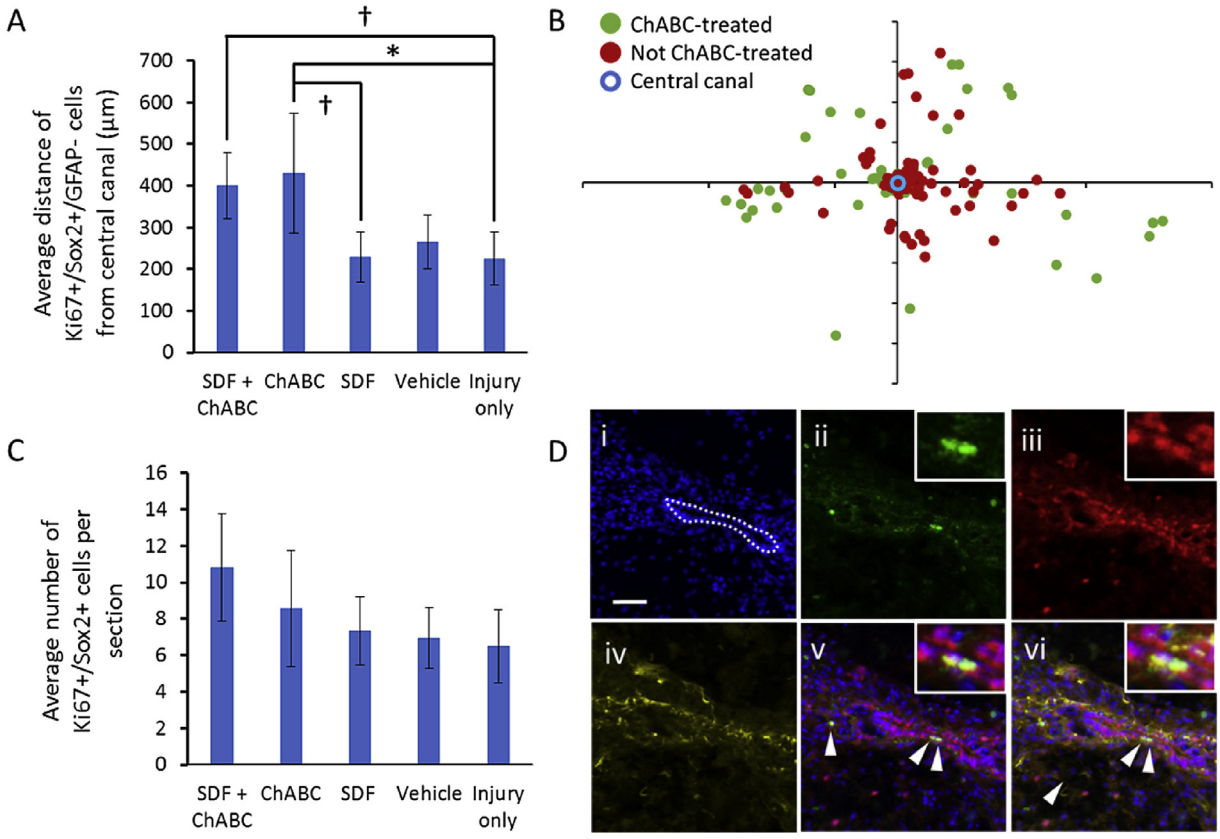


**Fig. 4. Treatment with ChABC increases distribution of NPCs throughout the spinal cord area**. A) ChABC significantly increases the average distance of NPCs from the central canal compared to SDF, vehicle, and injury only groups 2 weeks after injury. B) Distribution of all NPCs around the central canal. C) ChABC did not increase the total number of NPCs present 2 weeks after injury (n = 4 animals per group, mean ± SD plotted, †$p < 0.1$, *$p < 0.05$; significant differences by one-way ANOVA with Holm-Sidak's post-hoc test). D) Representative images of spinal cord tissue cross-section from the ChABC-treated group 2 weeks after injury showing i) DAPI (blue), ii) Ki67 (green), iii) Sox2 (red), iv) GFAP (yellow), v) overlay of DAPI/Sox2/Ki67 (white arrows show Sox2+/Ki67 + proliferating NPCs or astrocytes), vi) overlay of DAPI/Sox2/Ki67/GFAP (white arrows indicate Sox2+/Ki67+/GFAP- proliferating NPCs). Dotted line indicates central canal. Insets show zoomed images of the same two Sox2+/Ki67+/GFAP- cells. Scale bar = 27 μm. (For interpretation of the references to colour in this figure legend, the reader is referred to the web version of this article.)

NPCs to injury sites in the brain and spinal cord [7–9]. The combination of ChABC and SDF has not been tested in SCI previously.

We hypothesized that SDF would increase migration of endogenous NPCs to the injury site while degradation of the glial scar by CSPG would further enhance the distribution and survival of these cells, resulting in improved tissue and functional repair compared to either treatment alone. To test our hypothesis, we took advantage of innovative delivery strategies that allow independent and sustained, bioactive release of both factors to the injured cord [22,24,25].

We applied this dual controlled delivery system to rats with clip impact-compression injuries at the T1/T2 level and monitored behavioural recovery over eight weeks. Groups treated with ChABC, both alone and in combination with SDF, performed better on average at all timepoints, and were the only groups to show significant early and sustained within-group functional locomotor recovery over time when compared to one week post injury.

The behavioural improvements observed in the ChABC-treated groups are correlated with significantly lower CSPG levels and greater dispersion of NPCs within the tissue at the two-week timepoint. Although this study cannot definitively show causation, we hypothesize that both increased NPC dispersal and behavioural improvements are due to the decrease in CSPG, as observed in previous studies [15,35]. ChABC remains active within spinal cord tissue up to four days after a single injection [20] and its effects on CSPG levels last for up to ten days [36]. Based on previous studies, our system can achieve release of bioactive ChABC for at least seven days *in vitro*. Assuming a similar *in vivo* release profile, our hydrogel system can be expected to affect CSPG levels *in vivo* for approximately 20 days post injection. Indeed, we see concomitant behavioural improvements in the first few weeks after injury that persist throughout our 8 week study.

CSPG levels returned to control values at eight weeks post injury. Not surprisingly, our system was unable to decrease CSPG levels this long after injection. Multiple injections are a possibility, but it is undesirable to re-expose the injury site. Therefore, to extend the duration of behavioural improvement after a single injection of gel, the duration of ChABC release may need to be increased. Using our controlled release system, this can be achieved by increasing the concentration of SH3 binding peptide within the gel or changing the binding peptide to one with a stronger binding affinity [23]. In order to overcome ChABC instability over a longer time period, ChABC could be modified for improved stability by site-directed mutagenesis [37].

Another strategy is viral-mediated ChABC gene delivery to host cells [38,39]. Since the ChABC is secreted by host cells at the injury site, thermal instability is not an issue. Bartus et al. showed significant functional recovery in a rat model of SCI after viral delivery of ChABC [39]. Notwithstanding these exciting results, since Bartus et al. used a contusion model at T10/T11 and we used a clip compression model at T1/T2, a direct comparison cannot be made. Additionally, viral gene delivery still has significant challenges to

overcome, including the presence of neutralizing antibodies *in vivo*, immune-mediated elimination of transduced cells, and the potential lack of receptors for viral internalization on target cells [40].

Although other studies using ChABC treatment for SCI have shown significant behavioural recovery relative to controls [39,41,42], many have not shown improvement [43–45], and even fewer see these improvements in BBB scores, a gross measure of motor function. The largest improvements in BBB after ChABC treatment were shown by Caggiano et al. in a severe contusion injury model where the BBB score improved from 4 with control treatment to 8 within four weeks. Caggiano et al. also observed that the effect of ChABC treatment on BBB decreased with decreasing injury severity, perhaps because rats show considerable spontaneous recovery after mild injuries, often masking any beneficial effects of treatment [42]. The BBB scores observed in the present study are similar to those observed with Caggiano's mild injury, suggesting that the severity of the injury used here was insufficient to observe significant differences in a measure such as BBB score. In contrast, fine locomotor skills, such as foot faults and motor subscores, did show significant behavioural improvement within the ChABC groups, underscoring the benefit of this treatment strategy.

The timing of glial scar degradation is also an important factor in SCI treatments. Ablation of astrocytes, the main cellular component of the glial scar [46,47], or prevention of CSPG synthesis using xyloside [48] have been linked to negative effects such as increased cavity size and neuronal degeneration. In the acute injury phase, the glial scar has been suggested to stop the spread of damage [49]. Although ChABC is naturally delayed in its action, some studies have administered the enzyme in the sub-acute injury phase (four days post injury) in order to avoid possible negative effects [15,50]. While no differences in cavity size and number of GFAP-labelled astrocytes were observed between groups following acute administration of ChABC in this study, the positive effects of controlled release ChABC may be enhanced by administration in the sub-acute injury phase.

SDF treatment alone resulted in an increase in CSPG levels at two weeks, but not eight weeks, post injury. SDF is a potent monocyte chemoattractant and monocyte-derived macrophages also contribute to CSPG secretion within the injury site [51]. Additionally, astrocytes that are in close proximity to phagocytic cells have been shown to increase their CSPG production [52,53]. While no differences were seen in the number of GFAP-positive astrocytes nor in the number of ED1+ microglia/macrophages between groups, this does not preclude their role in the increased CSPG levels observed in the SDF group as microglia/macrophage numbers peak four to eight days after injury [54], which is earlier than our first timepoint. Since this increase in CSPG levels was not seen in the combined treatment group of SDF + ChABC, the degradation of CSPGs by ChABC is dominant over the effect of SDF.

We chose to co-deliver SDF because it is implicated in NPC migration in the spinal cord [9]. We therefore looked for proliferating NPCs based on co-expression of Ki67 and Sox2, but not GFAP (to exclude proliferating astrocytes). Since the clip compression injury model disrupts the central canal, where the multipotent endogenous stem cells of the spinal cord reside [5], dye-based prelabeling of the ependymal cell population was not possible. Instead, we examined tissue rostral and caudal to the injury epicenter where the central canal was still intact. In this study, we observed no differences in Ki67+/Sox2+/GFAP- cell numbers between groups and overall numbers of proliferating NPCs were very low. After SCI, the proliferation of endogenous spinal cord stem cells returns to baseline levels within two weeks [3] and migrating ependymal cells lose their expression of Sox2 by two weeks post injury and begin to differentiate [55]. Although we cannot conclude, based on these data, that SDF had no effect on NPC migration, we can conclude that any effect did not translate into significant functional improvement.

Interestingly, the average distance of proliferating NPCs from the central canal was significantly higher in ChABC treated groups, suggesting that ChABC enhances cell migration/distribution, which is consistent with other studies [14–16].

Overall, the beneficial tissue and functional outcomes observed in this study are solely due ChABC treatment. ChABC treatment reduced CSPG levels, enhanced NPC migration, and resulted in significantly improved within-group locomotor function over time. In addition, we demonstrated these benefits using a minimally invasive, local ChABC delivery system, in a clinically relevant, impact-compression injury model. While SDF did not impact regeneration the way we had anticipated, a different SCI model may be required to elucidate its effects and optimize its delivery. Despite these positive results, we recognize that ChABC treatment alone is insufficient for full functional recovery and thus, while SDF may not be the optimal factor for co-delivery with ChABC, other regenerative and/or neuroprotective factors may be required. The delivery system highlighted herein provides a convenient platform to test different combination strategies.

## Acknowledgements

We thank Mr. Peter Poon for performing all the surgeries and help with behavioural testing as well as Dr. Tobias Fuehrmann and Ms. Priya Anandakumaran for help with behavioural testing. We thank Dr. Andrea Mothe for helpful advice and discussions and Drs. Katarina Vulic and Roger Tam for help with material synthesis. We are grateful to funding from the Canadian Institutes of Health Research (FDN-143276) (Foundation grant to MSS), the Natural Sciences and Engineering Research Council of Canada (RGPIN-2014-04679) (Discovery to MSS, Vanier to MMP), and an Ontario Graduate Scholarship (to MMP).

## Appendix A. Supplementary data

Supplementary data related to this article can be found at http://dx.doi.org/10.1016/j.biomaterials.2017.04.016.

## References

[1] M. Kerschensteiner, M.E. Schwab, J.W. Lichtman, T. Misgeld, In vivo imaging of axonal degeneration and regeneration in the injured spinal cord, Nat. Med. 11 (2005) 572–577.
[2] V.J. Tom, M.P. Steinmetz, J.H. Miller, C.M. Doller, J. Silver, Studies on the development and behavior of the dystrophic growth cone, the hallmark of regeneration failure, in an in vitro model of the glial scar and after spinal cord injury, J. Neurosci. 24 (2004) 6531–6539.
[3] A.J. Mothe, C.H. Tator, Proliferation, migration, and differentiation of endogenous ependymal region stem/progenitor cells following minimal spinal cord injury in the adult rat, Neuroscience 131 (2005) 177–187. http://www.sciencedirect.com/science/article/pii/S0306452204009376.
[4] A. Jaerve, J. Schira, H.W. Muller, Concise review: The potential of stromal cell-derived factor 1 and its receptors to promote stem cell functions in spinal cord repair, Stem Cells Transl. Med. 1 (2012) 732–739.
[5] S. Weiss, C. Dunne, J. Hewson, C. Wohl, M. Wheatley, A.C. Peterson, B.A. Reynolds, Multipotent CNS stem cells are present in the adult mammalian spinal cord and ventricular neuroaxis, J. Neurosci. 16 (1996) 7599–7609.
[6] C.B. Johansson, S. Momma, D.L. Clarke, M. Risling, U. Lendahl, J. Frisén, Identification of a neural stem cell in the adult mammalian central nervous system, Cell. 96 (1999) 25–34.
[7] V.M. Tysseling, D. Mithal, V. Sahni, D. Birch, H. Jung, A. Belmadani, R.J. Miller, J.A. Kessler, SDF1 in the dorsal corticospinal tract promotes CXCR4+ cell migration after spinal cord injury, J. Neuroinflammation 8 (2011) 1742–2094.
[8] H. Takeuchi, A. Natsume, T. Wakabayashi, C. Aoshima, S. Shimato, M. Ito, J. Ishii, Y. Maeda, M. Hara, S.U. Kim, J. Yoshida, Intravenously transplanted human neural stem cells migrate to the injured spinal cord in adult mice in an SDF-1- and HGF-dependent manner, Neurosci. Lett. 426 (2007) 69–74. http://www.sciencedirect.com/science/article/pii/S0304394007009081.
[9] J. Imitola, K. Raddassi, K.I. Park, F.J. Mueller, M. Nieto, Y.D. Teng, D. Frenkel, J. Li, R.L. Sidman, C.A. Walsh, E.Y. Snyder, S.J. Khoury, Directed migration of

neural stem cells to sites of CNS injury by the stromal cell-derived factor 1alpha/CXC chemokine receptor 4 pathway, Proc. Natl. Acad. Sci. U. S. A. 101 (2004) 18117–18122.
[10] H. Peng, Y. Huang, J. Rose, D. Erichsen, S. Herek, N. Fujii, H. Tamamura, J. Zheng, Stromal cell-derived factor 1-mediated CXCR4 signaling in rat and human cortical neural progenitor cells, J. Neurosci. Res. 76 (2004) 35–50.
[11] A. Zendedel, M. Nobakht, M. Bakhtiyari, C. Beyer, M. Kipp, M. Baazm, M.T. Joghataie, Stromal cell-derived factor-1 alpha (SDF-1α) improves neural recovery after spinal cord contusion in rats, Brain Res. 1473 (2012) 214–226. http://www.sciencedirect.com/science/article/pii/S0006899312012267 (Accessed 13 September 2015).
[12] E.J. Bradbury, L.M. Carter, Manipulating the glial scar: chondroitinase ABC as a therapy for spinal cord injury, Brain Res. Bull. 84 (2011) 306–316.
[13] C. Bowes, J.M. Massey, M. Burish, C.M. Cerkevich, J.H. Kaas, Chondroitinase ABC promotes selective reactivation of somatosensory cortex in squirrel monkeys after a cervical dorsal column lesion, Proc. Natl. Acad. Sci. U. S. A. 109 (2012) 2595–2600.
[14] J. Ma, M. Kabiel, B.A. Tucker, J. Ge, M.J. Young, Combining chondroitinase ABC and growth factors promotes the integration of murine retinal progenitor cells transplanted into Rho(-/-) mice, Mol. Vis. 17 (2011) 1759–1770.
[15] S. Karimi-Abdolrezaee, E. Eftekharpour, J. Wang, D. Schut, M.G. Fehlings, Synergistic effects of transplanted adult neural stem/progenitor cells, chondroitinase, and growth factors promote functional repair and plasticity of the chronically injured spinal cord, J. Neurosci. 30 (2010) 1657–1676.
[16] H. Kanno, Y. Pressman, A. Moody, R. Berg, E.M. Muir, J.H. Rogers, H. Ozawa, E. Itoi, D.D. Pearse, M.B. Bunge, Combination of engineered schwann cell grafts to secrete neurotrophin and chondroitinase promotes axonal regeneration and locomotion after spinal cord injury, J. Neurosci. 34 (2014) 1838–1855.
[17] H. Peng, Y.M. Wu, Z.Y. Duan, P. Ciborowski, J.L.C. Zheng, Proteolytic processing of SDF-1 alpha by matrix metalloproteinase-2 impairs CXCR4 signaling and reduces neural progenitor cell migration, Protein Cell. 3 (2012) 875–882.
[18] J. Yang, G. Wang, C. Gao, G. Shao, N. Kang, Effects of hyperbaric oxygen on MMP-2 and MMP-9 expressions and spinal cord edema after spinal cord injury, Life Sci. 93 (2013) 1033–1038.
[19] N.J. Tester, A.H. Plaas, D.R. Howland, Effect of body temperature on chondroitinase ABC's ability to cleave chondroitin sulfate glycosaminoglycans, J. Neurosci. Res. 85 (2007) 1110–1118.
[20] D. Crespo, R.A. Asher, R. Lin, K.E. Rhodes, J.W. Fawcett, How does chondroitinase promote functional recovery in the damaged CNS? Exp. Neurol. 206 (2007) 159.
[21] K.A. Follett, R.L. Boortz-Marx, J.M. Drake, S. DuPen, S.J. Schneider, M.S. Turner, R.J. Coffey, Prevention and management of intrathecal drug delivery and spinal cord stimulation system infections, Anesthesiology 100 (2004) 1582–1594.
[22] M.M. Pakulska, K. Vulic, M.S. Shoichet, Affinity-based release of chondroitinase ABC from a modified methylcellulose hydrogel, J. Control. Release 171 (2013) 11–16.
[23] K. Vulic, M.M. Pakulska, R. Sonthalia, A. Ramachandran, M.S. Shoichet, Mathematical model accurately predicts protein release from an affinity-based delivery system, J. Control. Release 197 (2015) 69–77.
[24] M.M. Pakulska, I. Elliott Donaghue, J.M. Obermeyer, A. Tuladhar, C.K. McLaughlin, T.N. Shendruk, M.S. Shoichet, Encapsulation-free controlled release: electrostatic adsorption eliminates the need for protein encapsulation in PLGA nanoparticles, Sci. Adv. 2 (2016).
[25] M.M. Pakulska, K. Vulic, R.Y. Tam, M.S. Shoichet, Hybrid crosslinked methylcellulose hydrogel: a predictable and tunable platform for local drug delivery, Adv. Mater. 27 (2015) 5002–5008.
[26] K. Vulic, M.S. Shoichet, Tunable growth factor delivery from injectable hydrogels for Tissue engineering, J. Am. Chem. Soc. 134 (2011) 882–885.
[27] M.D. Baumann, C.E. Kang, C.H. Tator, M.S. Shoichet, Intrathecal delivery of a polymeric nanocomposite hydrogel after spinal cord injury, Biomaterials 31 (2010) 7631–7639.
[28] P.C. Poon, D. Gupta, M.S. Shoichet, C.H. Tator, Clip compression model is useful for thoracic spinal cord injuries: histologic and functional correlates, Spine (Phila. Pa. 1976) 32 (2007) 2853–2859.
[29] D.M. Basso, M.S. Beattie, J.C. Bresnahan, A sensitive and reliable locomotor rating scale for open field Testing in rats, J. Neurotrauma 12 (2009) 1.
[30] A.J. Lankhorst, M.R. Verzijl, F.P.T. Hamers, Experimental spinal cord contusion injury: comparison of different outcome parameters, Neurosci. Res. Commun. 24 (1999) 135.
[31] G.A. Metz, I.Q. Whishaw, Cortical and subcortical lesions impair skilled walking in the ladder rung walking test: a new task to evaluate fore- and hindlimb stepping, placing, and co-ordination, J. Neurosci. Methods 115 (2002) 169–179.
[32] J. Schindelin, I. Arganda-Carreras, E. Frise, V. Kaynig, M. Longair, T. Pietzsch, S. Preibisch, C. Rueden, S. Saalfeld, B. Schmid, J.-Y. Tinevez, D.J. White, V. Hartenstein, K. Eliceiri, P. Tomancak, A. Cardona, Fiji: an open-source platform for biological-image analysis, Nat. Methods 9 (2012) 676–682.
[33] C.E. Kang, M.D. Baumann, C.H. Tator, M.S. Shoichet, Localized and sustained delivery of fibroblast growth factor-2 from a nanoparticle-hydrogel composite for treatment of spinal cord injury, Cells Tissues Organs 197 (2013) 55–63.
[34] I. Elliott Donaghue, C.H. Tator, M.S. Shoichet, Sustained delivery of bioactive neurotrophin-3 to the injured spinal cord, Biomater. Sci. 3 (2015) 65–72.
[35] R. Mckeon, A. Höke, J. Silver, Injury-induced proteoglycans inhibit the potential for laminin-mediated axon growth on astrocytic scars, Exp. Neurol. 136 (1995) 32–43.
[36] R. Lin, J.C.F. Kwok, D. Crespo, J.W. Fawcett, Chondroitinase ABC has a long-lasting effect on chondroitin sulphate glycosaminoglycan content in the injured rat brain, J. Neurochem. 104 (2008) 400.
[37] M. Nazari-Robati, K. Khajeh, M. Aminian, N. Mollania, A. Golestani, Enhancement of thermal stability of chondroitinase ABC I by site-directed mutagenesis: an insight from Ramachandran plot, Biochim. Biophys. Acta - Proteins Proteom. 1834 (2013) 479–486.
[38] R.R. Zhao, E.M. Muir, J.N. Alves, H. Rickman, A.Y. Allan, J.C. Kwok, K.C.D. Roet, J. Verhaagen, B.L. Schneider, J.C. Bensadoun, S.G. Ahmed, R.J. Yanez-Munoz, R.J. Keynes, J.W. Fawcett, J.H. Rogers, Lentiviral vectors express chondroitinase ABC in cortical projections and promote sprouting of injured corticospinal axons, J. Neurosci. Methods 201 (2011) 228–238.
[39] K. Bartus, N.D. James, A. Didangelos, K.D. Bosch, J. Verhaagen, R.J. Yanez-Munoz, J.H. Rogers, B.L. Schneider, E.M. Muir, E.J. Bradbury, Large-scale chondroitin sulfate proteoglycan digestion with chondroitinase gene therapy leads to reduced pathology and modulates macrophage phenotype following spinal cord contusion injury, J. Neurosci. 34 (2014) 4822–4836.
[40] M.A. Kotterman, D.V. Schaffer, Engineering adeno-associated viruses for clinical gene therapy, Nat. Rev. Genet. 15 (2014) 445–451.
[41] E.J. Bradbury, L.D.F. Moon, R.J. Popat, V.R. King, G.S. Bennett, P.N. Patel, J.W. Fawcett, S.B. McMahon, Chondroitinase ABC promotes functional recovery after spinal cord injury, Nature 416 (2002) 636–640.
[42] A.O. Caggiano, M.P. Zimber, A. Ganguly, A.R. Blight, E.A. Gruskin, Chondroitinase ABCI improves locomotion and bladder function following contusion injury of the rat spinal cord, J. Neurotrauma 22 (2005) 226–239.
[43] Y.G. Yang, D.M. Jiang, Z.X. Quan, Y.S. Ou, Insulin with chondroitinase ABC treats the rat model of acute spinal cord injury, J. Int. Med. Res. 37 (2009) 1097–1107.
[44] H. Lee, R.J. McKeon, R.V. Bellamkonda, Sustained delivery of thermostabilized chABC enhances axonal sprouting and functional recovery after spinal cord injury, Proc. Natl. Acad. Sci. 107 (2010) 3340–3345.
[45] A. Mountney, M.R. Zahner, E.R. Sturgill, C.J. Riley, J.W. Aston, M. Oudega, L.P. Schramm, A. Hurtado, R.L. Schnaar, Sialidase, chondroitinase ABC, and combination therapy after spinal cord contusion injury, J. Neurotrauma 30 (2013) 181–190.
[46] J.R. Faulkner, J.E. Herrmann, M.J. Woo, K.E. Tansey, N.B. Doan, M. V Sofroniew, Reactive astrocytes protect Tissue and preserve function after spinal cord injury, J. Neurosci. 24 (2004) 2143–2155.
[47] H. Sabelstrom, M. Stenudd, P. Reu, D.O. Dias, M. Elfineh, S. Zdunek, P. Damberg, C. Goritz, J. Frisen, Resident neural stem cells restrict tissue damage and neuronal loss after spinal cord injury in mice, Science (80-.) 342 (2013) 637–640.
[48] A. Rolls, R. Shechter, A. London, Y. Segev, J. Jacob-Hirsch, N. Amariglio, G. Rechavi, M. Schwartz, Two faces of chondroitin sulfate proteoglycan in spinal cord repair: a role in microglia/macrophage activation, PLoS Med. 5 (2008) e171.
[49] A. Rolls, R. Shechter, M. Schwartz, The bright side of the glial scar in CNS repair, Nat. Rev. Neurosci. 10 (2009) 235–241.
[50] S. Karimi-Abdolrezaee, D. Schut, J. Wang, M.G. Fehlings, Chondroitinase and growth factors enhance activation and oligodendrocyte differentiation of endogenous neural precursor cells after spinal cord injury, PLoS One 7 (2012) e37589.
[51] M.G. Fehlings, A.R. Vaccaro, M. Boakye, S. Rossignol, J.F. Ditunno Jr., A.S. Burns (Eds.), Essentials of Spinal Cord Injury: Basic Research to Clinical Practice, 2012. Thieme.
[52] M.T. Fitch, J. Silver, Activated macrophages and the blood-brain barrier: inflammation after CNS injury leads to increases in putative inhibitory molecules, Exp. Neurol. 148 (1997) 587–603.
[53] M.T. Fitch, C. Doller, C.K. Combs, G.E. Landreth, J. Silver, Cellular and molecular mechanisms of glial scarring and progressive cavitation: in vivo and in vitro analysis of inflammation-induced secondary injury after CNS trauma, J. Neurosci. 19 (1999) 8182–8198.
[54] I. Dusart, M.E. Schwab, Secondary cell death and the inflammatory reaction after dorsal hemisection of the rat spinal cord, Eur. J. Neurosci. 6 (1994) 712–724.
[55] F. Barnabe-Heider, C. Goritz, H. Sabelstrom, H. Takebayashi, F.W. Pfrieger, K. Meletis, J. Frisen, Origin of new glial cells in intact and injured adult spinal cord, Cell Stem Cell. 7 (2010) 470–482.